Microscopic Nuclei Classification, Segmentation, and Detection with improved Deep Convolutional Neural Networks (DCNN)

Md Zahangir Alom (malom@stjude.org)
St Jude Children's Research Hospital https://orcid.org/0000-0002-2314-1207
Vijayan K. Asari
University of Dayton
Anil Parwani
The Ohio State University
Tarek M. Taha
University of Dayton

Research

Keywords: Digital pathology, Nuclei detection, Nuclei segmentation, DRCN, R2U-Net, UD-Net

Posted Date: May 24th, 2021

DOI: https://doi.org/10.21203/rs.3.rs-506324/v1

Version of Record: A version of this preprint was published at Diagnostic Pathology on April 19th, 2022.
See the published version at https://doi.org/10.1186/s13000-022-01189-5.

Abstract

Background

Nuclei classification, segmentation, and detection from pathological images are challenging tasks due to cellular heterogeneity in the Whole Slide Images (WSI).

Methods

In this work, we propose advanced DCNN models for nuclei classification, segmentation, and detection tasks. The Densely Connected Neural Network (DCNN) and Densely Connected Recurrent Convolutional Network

(DCRN) models are applied for the nuclei classification tasks. The Recurrent Residual U-Net (R2U-Net) and the R2UNet-based regression model named as the University of Dayton Net (UD-Net) are applied for nuclei segmentation and detection tasks respectively.The experiments are conducted on publicly available datasets including Routine Colon Cancer (RCC) classification and detection and the Nuclei Segmentation Challenge 2018 datasets for segmentation task. The performance of the proposed methods is compared against the existing approaches in terms of precision, recall, Dice Coefficient (DC), Mean Squared Error (MSE), F1-score, and overall testing accuracy by performing pixels and cell-level analysis.

Results

The experimental results demonstrate around 2.2% and 4.5% higher performance in terms of F1-score for nuclei classification and detection tasks when compared to the recently published DCNN based method. Also, for nuclei segmentation, the R2U-Net shows around 91.63% testing accuracy in terms of DC which is around 0.76% higher compared to the U-Net model.

Conclusion

The proposed methods demonstrate robustness with better quantitative and qualitative results in three different tasks for analyzing the WSI.

Full Text

This preprint is available for download as a PDF.

Figures

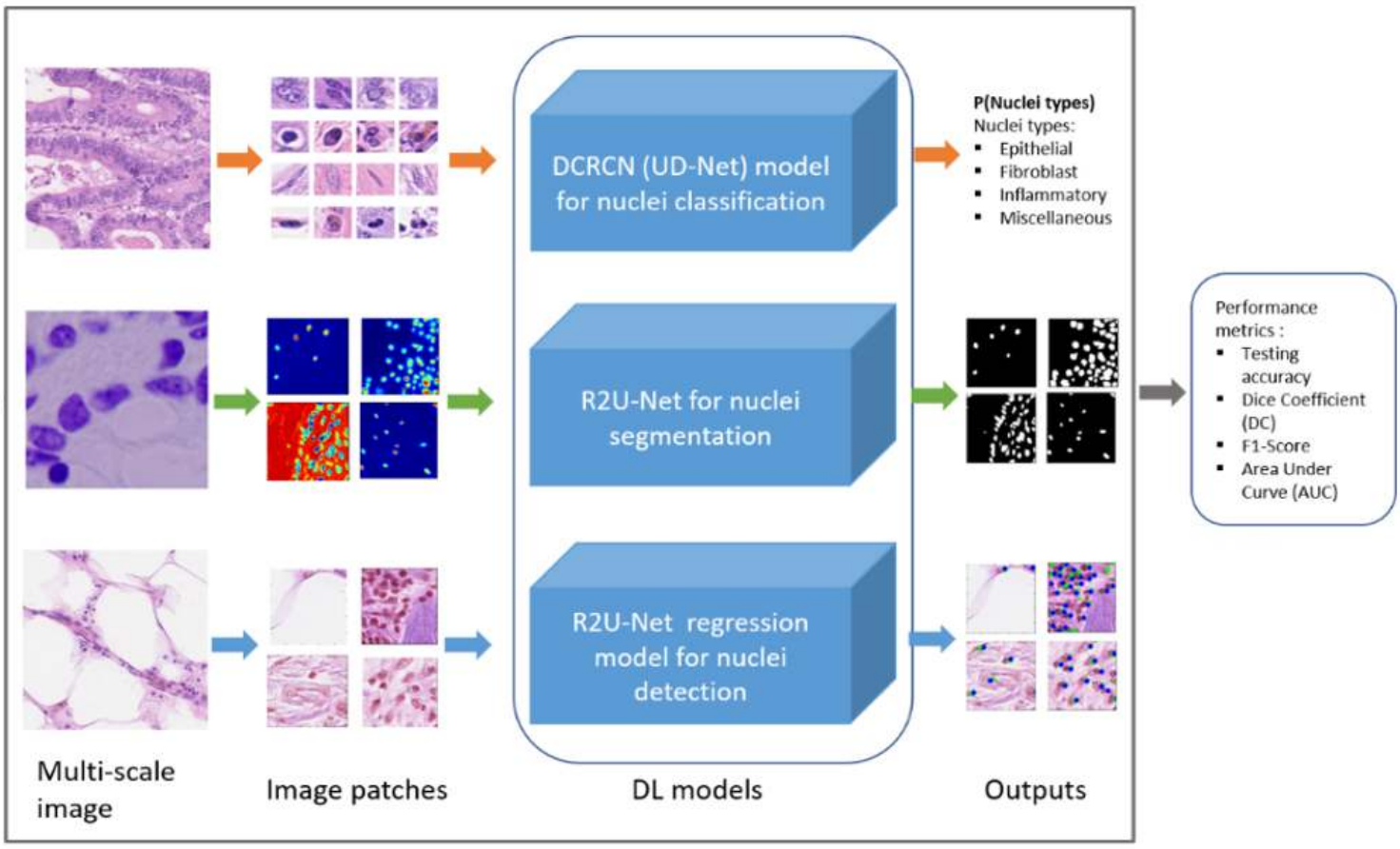

Figure 1

Proposed system: the patches are extracted from the multi-scale slide as required. Three different DL models are applied for nuclei classification, segmentation, and detection tasks. Finally, the performance is evaluated with different performance metrics.

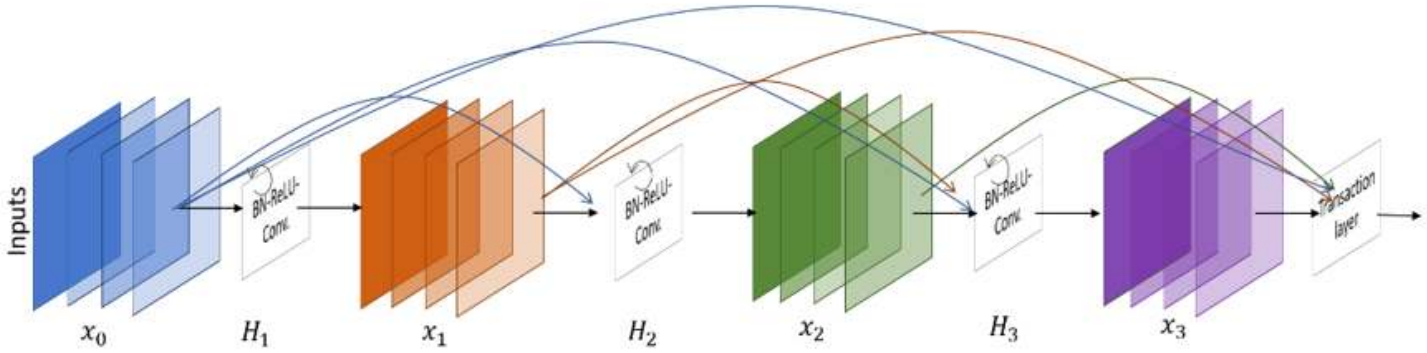

Figure 2

The Densely Connected Recurrent Network model with recurrent, convolutional, and transition blocks.

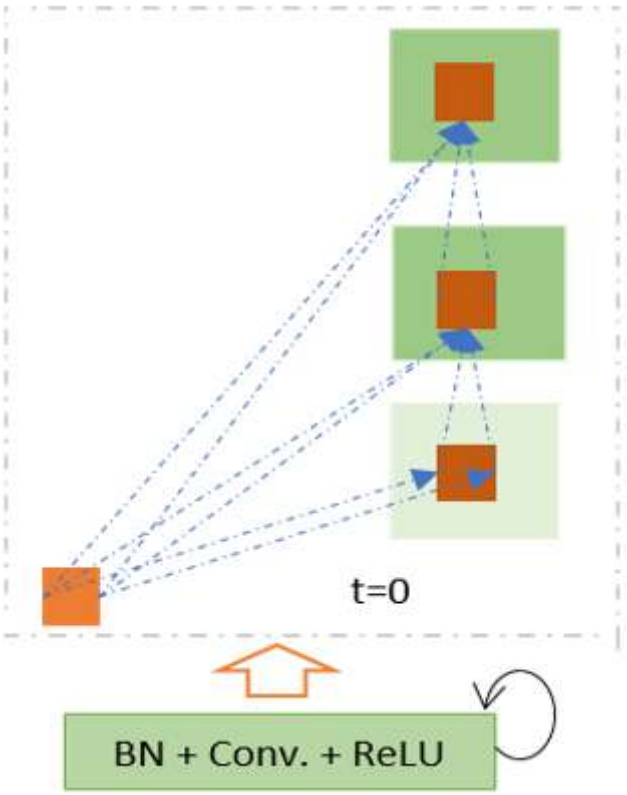

Figure 3

Unfolded recurrent convolutional layer for time step t = 2.

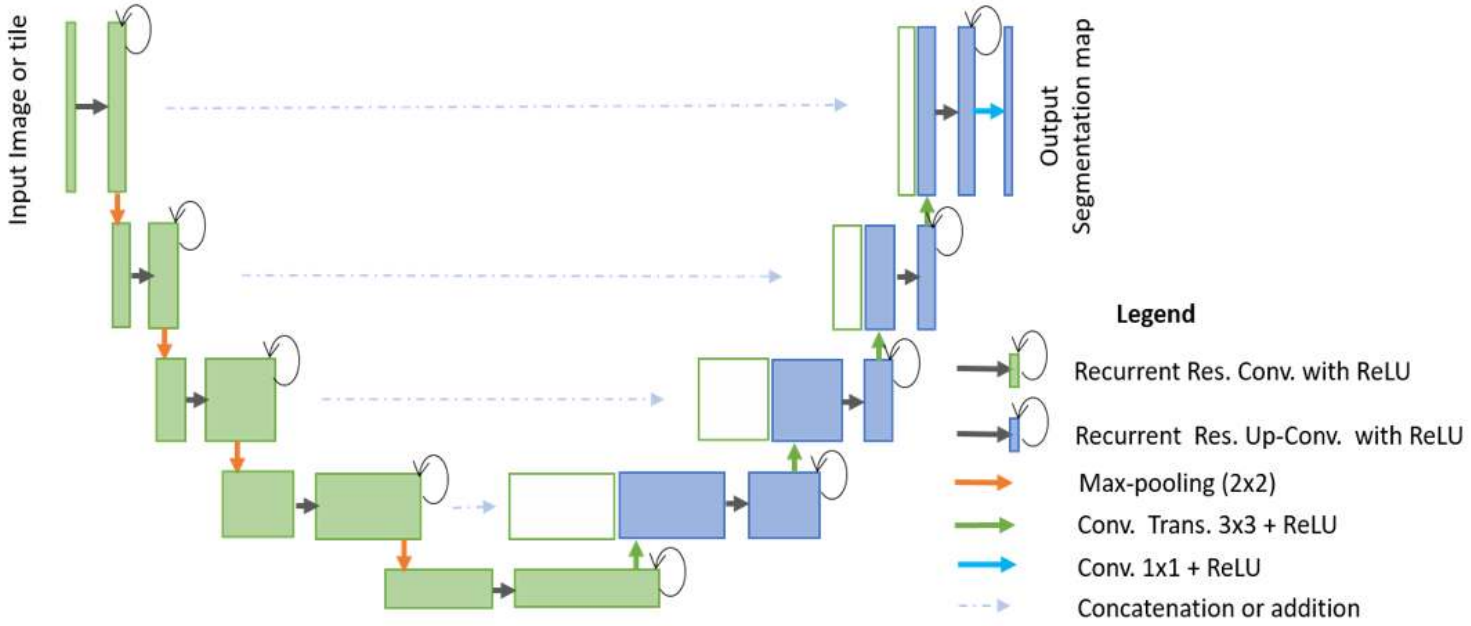

Figure 4

Diagram displaying end-to-end nuclei segmentation using the R2U-Net model where the green part refers to the encoding unit, and the blue part refers to the decoding units.

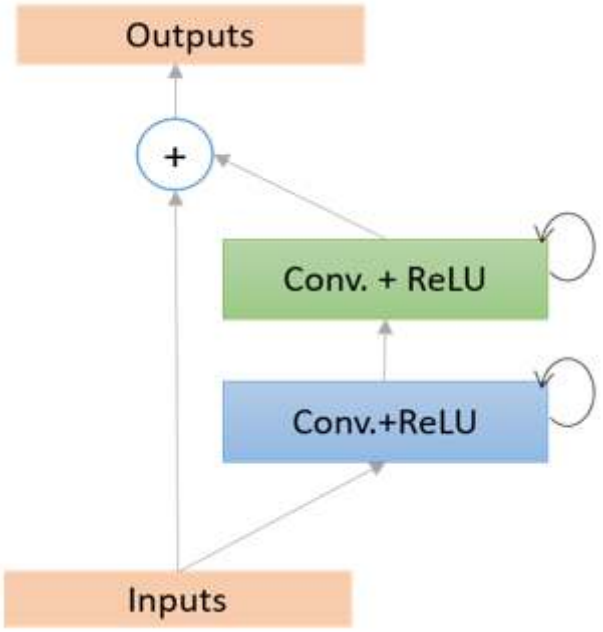

Figure 5

The recurrent residual unit (RRU) for both R2U-Net and UD-Net models.

Figure 6

Example images from the dataset for nuclei classification.

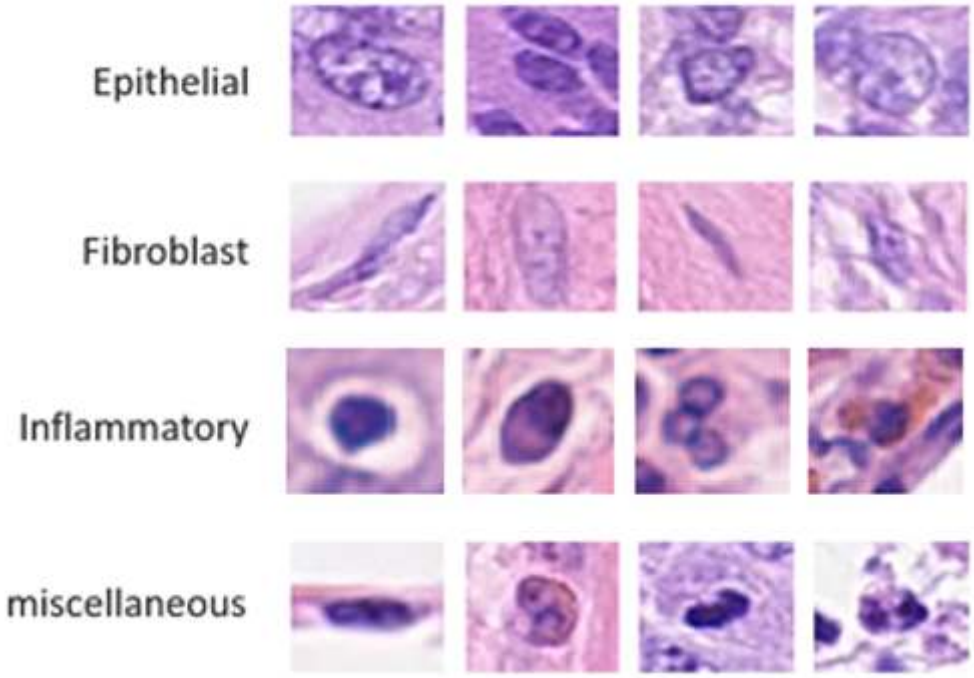

Figure 7

Randomly selected patches for four different types of nuclei of routine colon cancer.

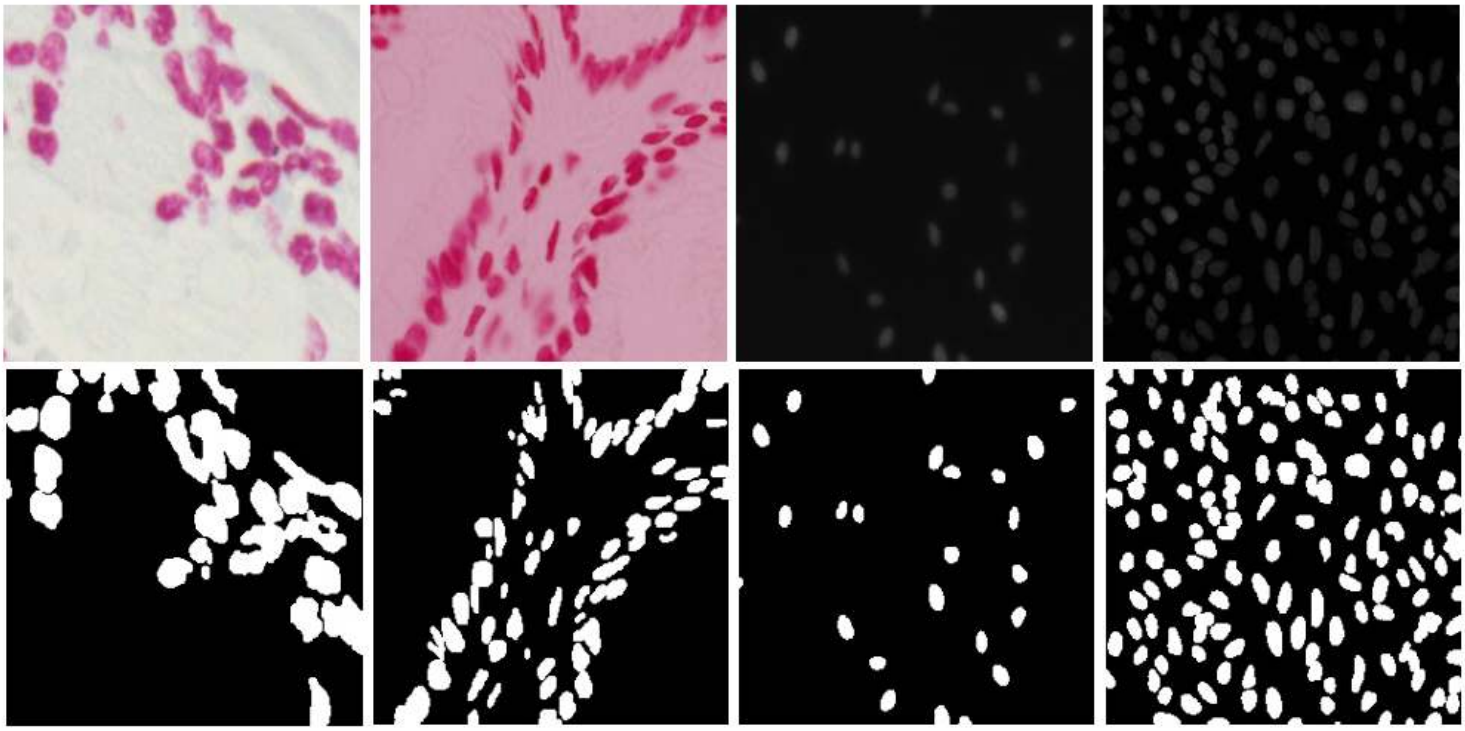

Figure 8

Example input images with segmentation masks: the first row shows input samples and the pixel label annotated masks are shown in the second row.

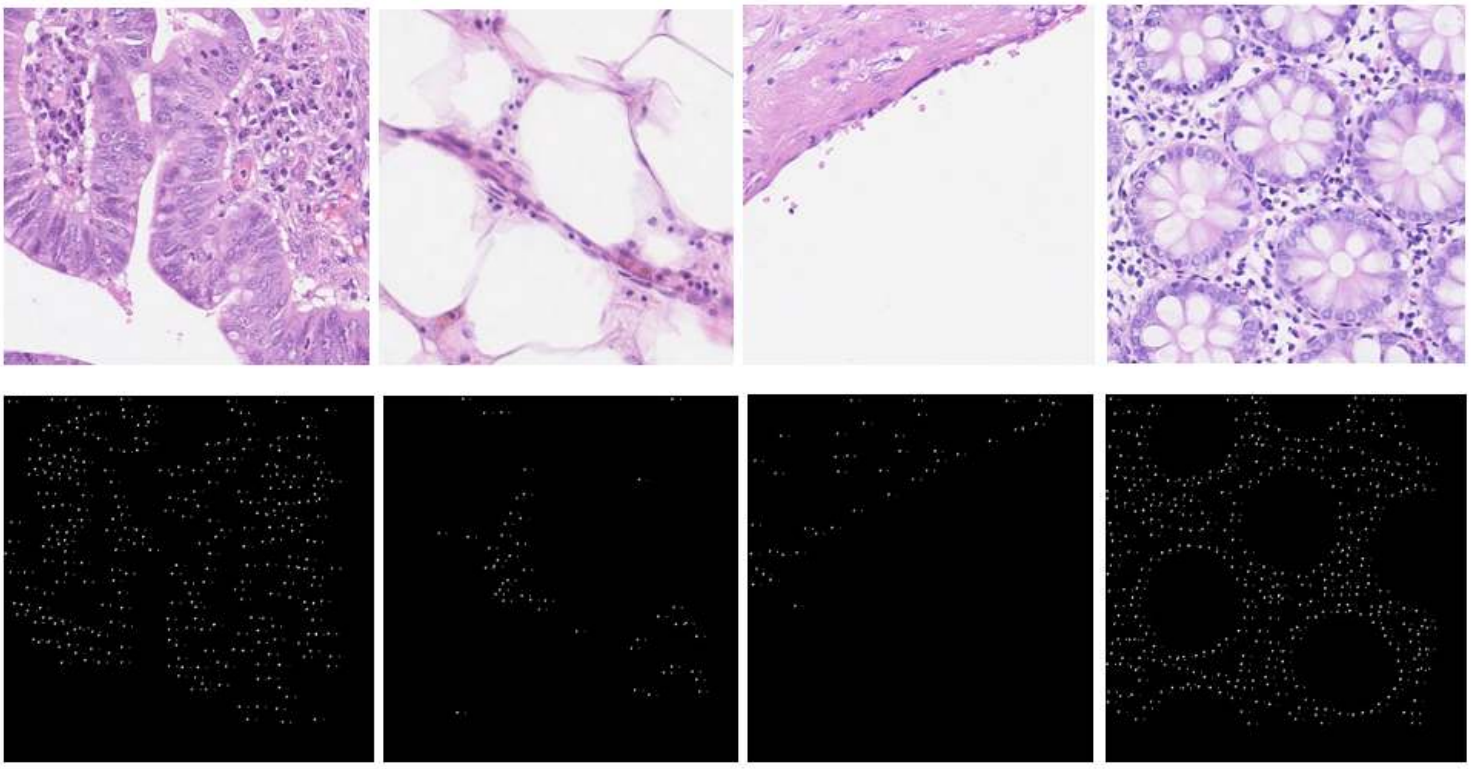

Figure 9

Randomly selected input images are shown in the first row and corresponding dilated masks with 3x3 kernels are shown on the second row for nuclei detection tasks.

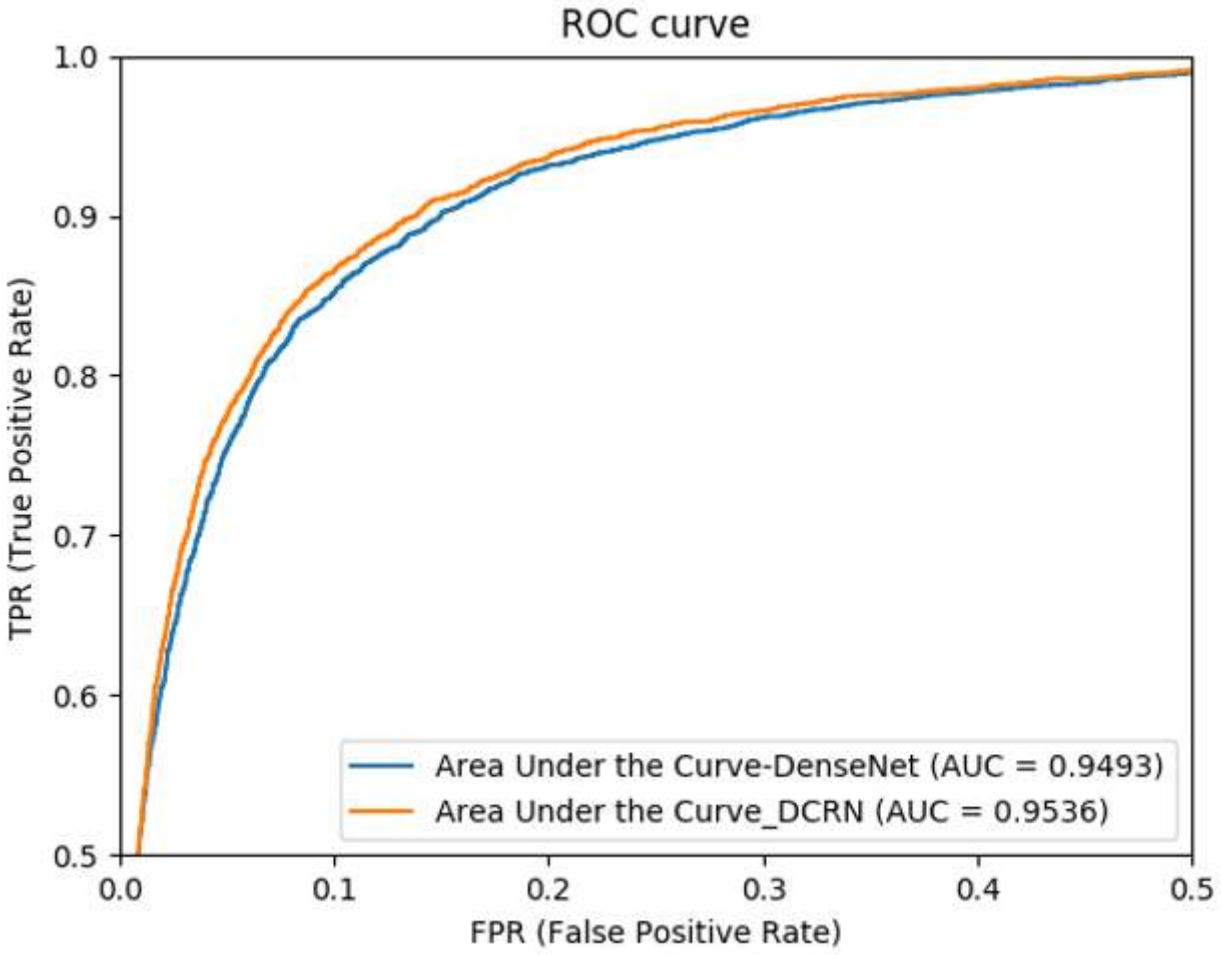

Figure 10

Area under the ROC curve of the DenseNet and DCRN models for nuclei classification tasks.

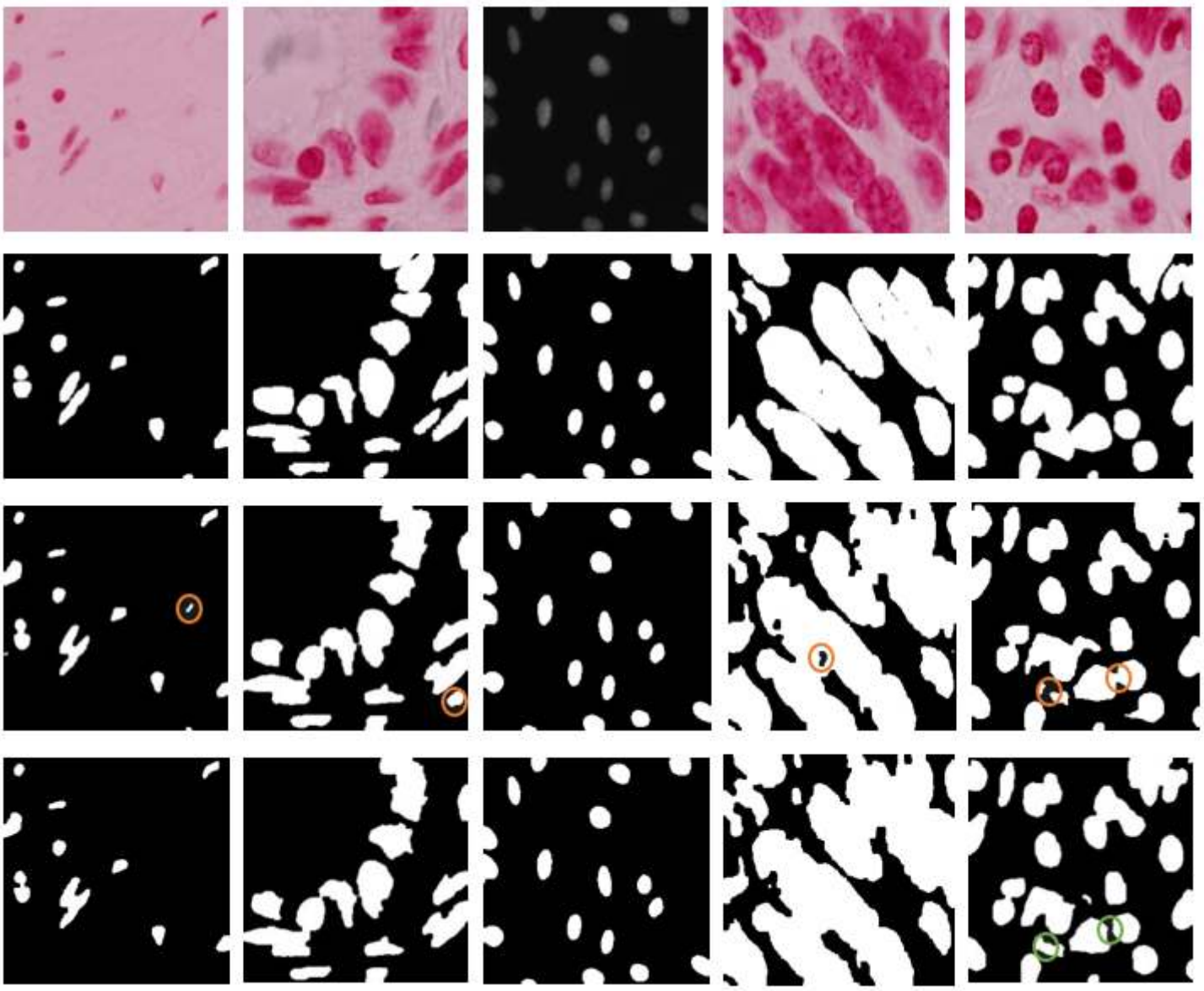

Figure 11

Qualitative results for both U-Net and R2U-Net models for nuclei segmentation, the first row shows the input samples, the second row shows the corresponding ground truth masks, the third and third row shows the outputs for U-Net and the fourth row show the outputs from R2U-Net model. The orange circles show the false detection of the U-Net model.

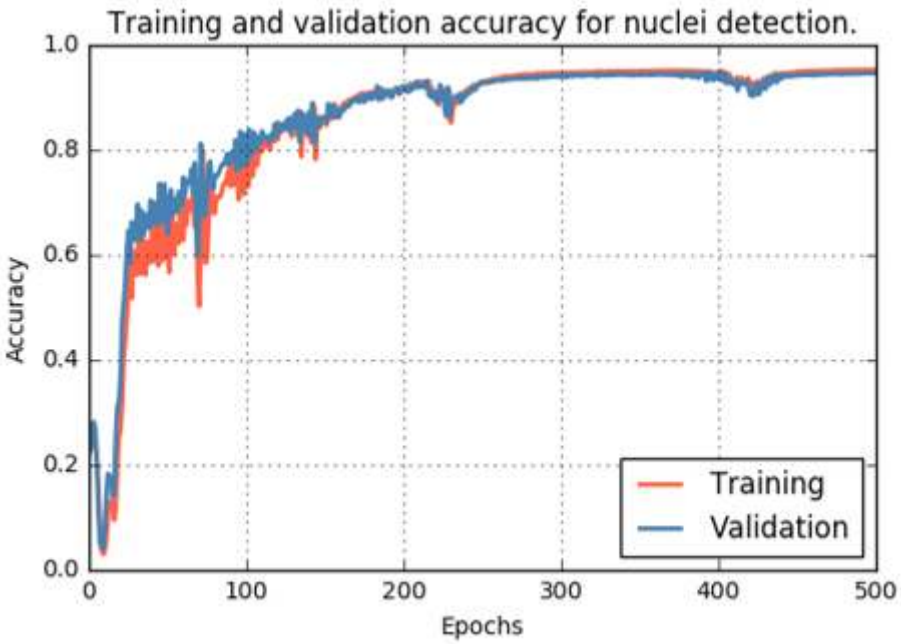

Figure 12

Training and validation accuracy of the UD-Net model for nuclei detection.

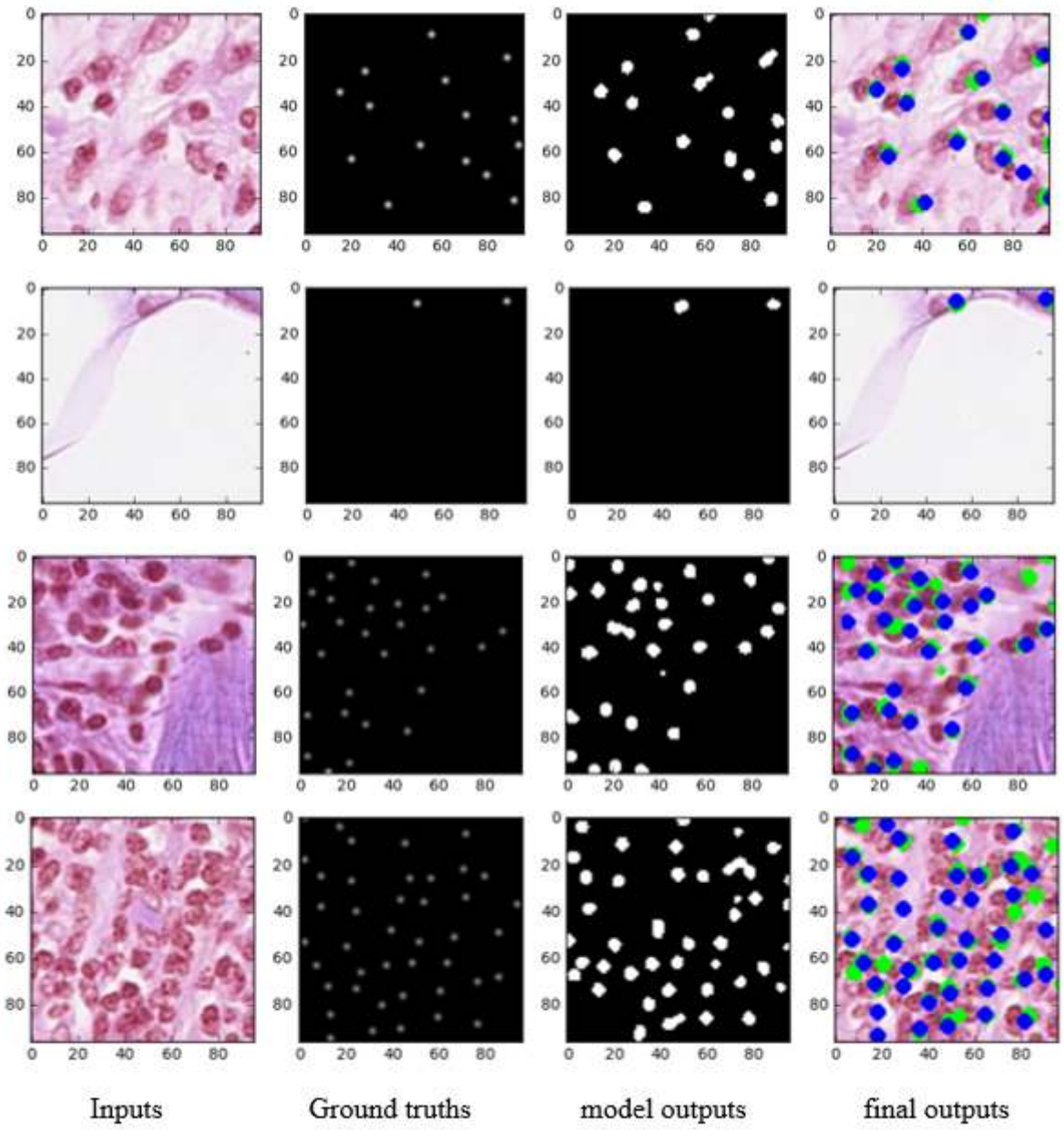

Figure 13

Nuclei detection outputs with inputs, ground truth, model outputs after thresholding, and final outputs with a blue and green dot. The blue dot represents the ground truth and the green dot shows the center pixels of the network outputs.

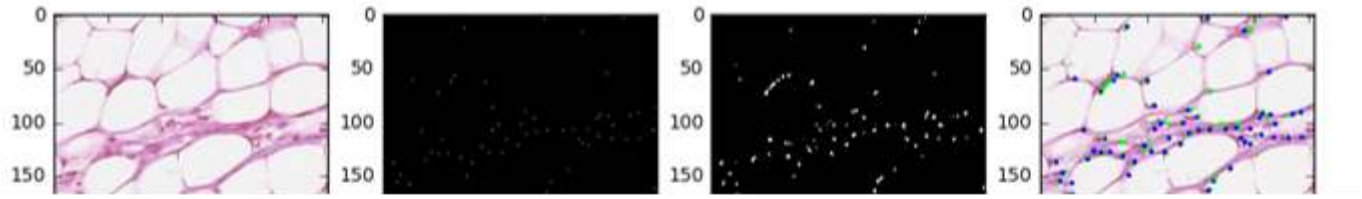

Figure 14

Nuclei detection output images generated from the output patches.